Supporting Information

Exploring the degradation mechanism of nickel-copper-molybdenum hydrogen evolution catalyst during intermittent operation

Shengxiong Yang,[a] Zhihan Liu,[a] Pengcheng Wan,[b] Liangsheng Liu,[a] Yimin Sun,[b] Fei Xiao,*[a] Shuai Wang*[a] and Junwu Xiao*[a]

[a]Key Laboratory of Material Chemistry for Energy Conversion and Storage, Ministry of Education, Hubei Key Laboratory of Material Chemistry and Service Failure, Department of Chemistry and Chemical Engineering, Huazhong University of Science and Technology, Wuhan 430074, China.

E-mail: xiaofei@hust.edu.cn, chmsamuel@hust.edu.cn, chjwxiao@hust.edu.cn

[b]Hubei key Laboratory of Plasma Chemistry and Advanced Materials, School of Materials Science and Engineering, Wuhan Institute of Technology, Wuhan, 430205, China.

Experimental Section

Trimetallic Ni–Cu–Mo catalyst was synthesized via a two-step precipitation-reduction method with modification of prior reports.[1, 2] Briefly, 3.6 mmol $Ni(NO_3)_2 \cdot 6H_2O$ and 0.4 mmol $Cu(NO_3)_2 \cdot 3H_2O$ were dissolved in 10 ml deionized water and then 4 ml of 25% ammonia solution was added to the solution. Following that, 0.57 mmol $(NH_4)_6Mo_7O_{24} \cdot 4H_2O$ (Ni/Cu/Mo = 9/1/10) and 100 g diethylene glycol were added to the mixture in steps. The reaction solution was then heated at 110°C for 40 min to yield a green solid. Subsequently, the green solid was annealed at 500°C for 1 h under 10% H_2/N_2. The $Ni_xCu_{1-x}Mo$ ($0 \leqslant x \leqslant 1$) composition was modulated by varying the molar ratio of metal salt precursors.

Self-supported $NiMoO_x$ and $CoMoO_x$ electrodes were synthesized using $Ni(NO_3)_2 \cdot 6H_2O$ or $Co(NO_3)_2 \cdot 6H_2O$ and $(NH_4)_6Mo_7O_{24} \cdot 4H_2O$ precursors through hydrothermal method followed by the thermal decomposition, according to the previous literature.[3, 4]

Characterization

Morphologies of the samples were examined by SEM (Hitachi SU8010 field-emission scanning electron microscopy) and TEM (FEI Tecnai G2 F30 transmission electron microscope). X-ray diffraction (XRD) patterns were collected on a Rigaku SmartLab SE. X-ray photoelectron spectroscopy (XPS) was performed on a Kratos AXIS Supra X-ray photoelectron spectrometer equipped with an Al Kα radiation source. Raman spectra were recorded on an Ostec-ArtTool Ramos S120 Raman spectroscope with 532 nm wavelength laser excitation. Concentrations of metal dissolution were determined by ICP-OES (Thermofisher iCAP7200plus spectrometer).

Electrochemical Measurements

A standard three-electrode set-up was used for the HER electrochemical measurements with a CHI 760E electrochemical workstation in 1.0 M KOH electrolyte. A graphite rod used as the counter electrode and a Hg/HgO electrode as the reference electrode. The catalyst was loaded onto a glassy carbon electrode with a loading of 0.2 mg cm^{-2}. All potentials were obtained against the reversible hydrogen electrode (RHE). Linear sweep voltammograms (LSV) were recorded by scanning from 0.05 V to -0.40 V versus RHE with a scan rate of 5 mV s^{-1}. All electrochemical data were collected without *iR* compensation. To effectively detect the concentration of dissolved metal ions in the electrolyte during continuous and intermittent operations, the catalyst was sprayed onto a carbon paper (TGP-H-060, 10% wet proof) with a loading of 4 mg cm^{-2}.

Fabrication and Test of the HEMELs

The HEMEL single cell consists of cathode, HEM, anode, gas diffusion layers (GDL), and flow field plates. The cathode catalyst ink was prepared by mixing Ni–Cu–Mo powder (40 mg), ionomer solution (110 mg, 5% in ethanol), deionized water (0.2 g), and isopropyl alcohol (0.8 g). The ink was sonicated for 1 h before spraying onto a PiperION^{TM} HEM using an airbrush (Iwata, Japan). Carbon paper (TGP-H-060, 10% wet proof) was used as the gas diffusion layer (GDL) in the cathode. Our previously reported self-supported FeNiOOH(F) covered with PiperION^{TM} ionomer was employed as the anode.[5] The area of membrane-electrode-assembly (MEA) was 5 cm^2. 1.0 M KOH solution or deionized water (18.2 MΩ cm) was pumped to the anode at a flow rate of 30 mL min^{-1}. The cell potential and high frequency resistance (HFR) of the HEMELs were recorded by a home-made flow electrolyzer test station.

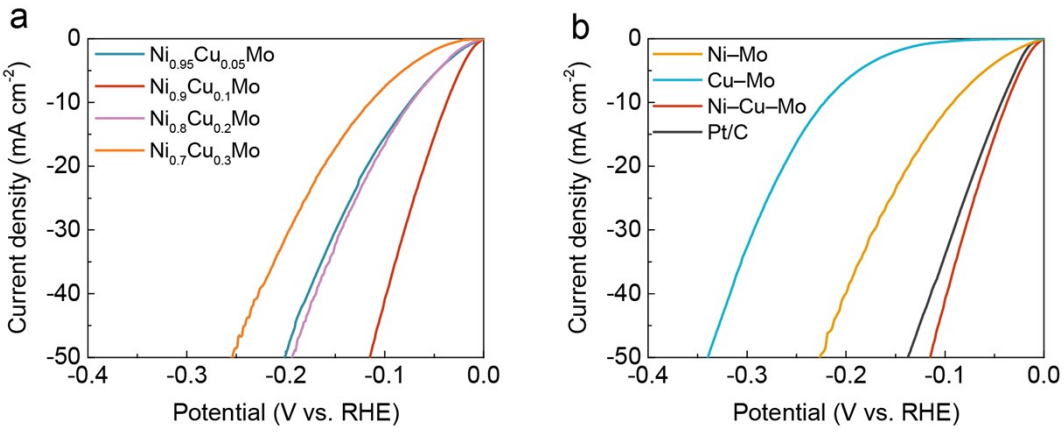

Fig. S1 (a) The HER polarization curves of the $Ni_xCu_{1-x}Mo$ catalysts measured in 1.0 M KOH solution. (b) The HER polarization curves of the Ni–Mo, Cu–Mo, Ni–Cu–Mo and commercial Pt/C (20 wt%) in 1.0 M KOH electrolyte without *iR* compensation.

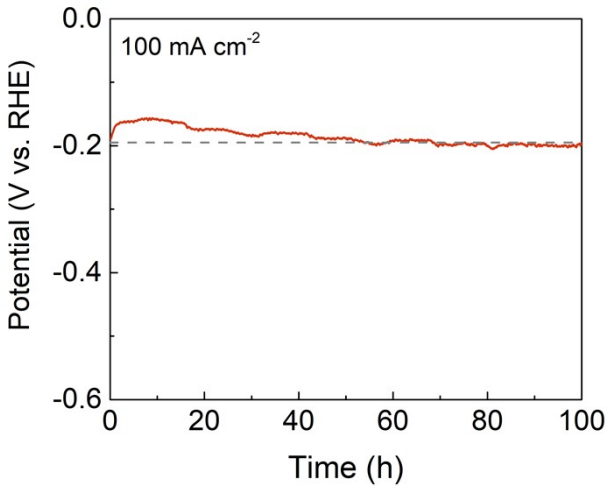

Fig. S2 Chronopotentiometry curve of the Ni–Cu–Mo catalyst at 100 mA cm^{-2} in 1.0 M KOH solution.

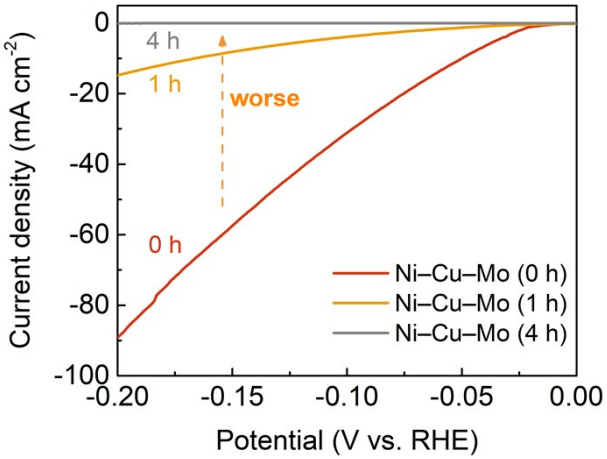

Fig. S3 LSV curves of the Ni–Cu–Mo catalyst after 0-4 hours of power off intervals.

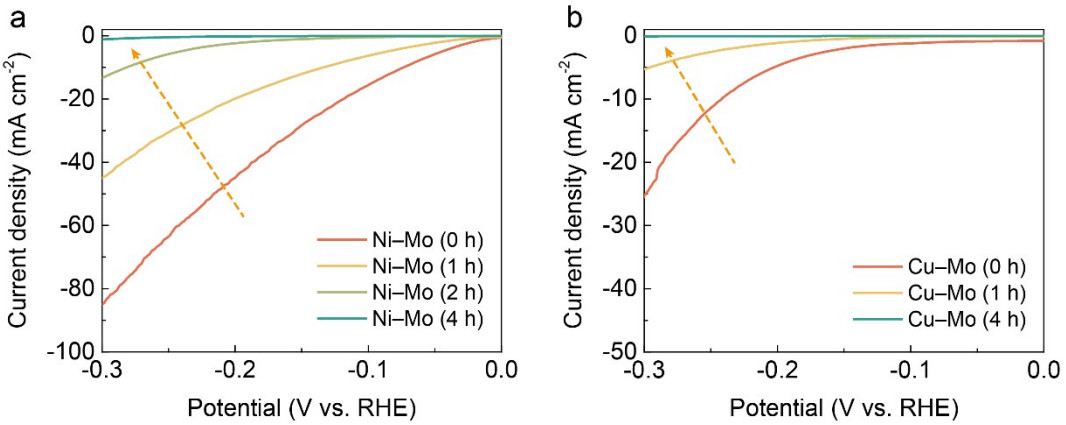

Fig. S4 LSV curves of the (a) Ni–Mo and (b) Cu–Mo catalysts after 0-4 hours of power off intervals.

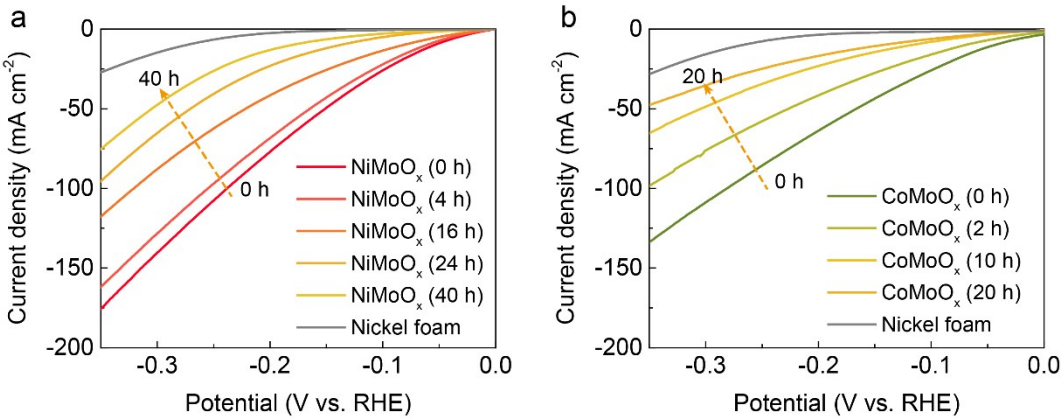

Fig. S5 LSV curves of self-supported (a) $NiMoO_x$ and (b) $CoMoO_x$ electrodes after several hours of power off intervals.

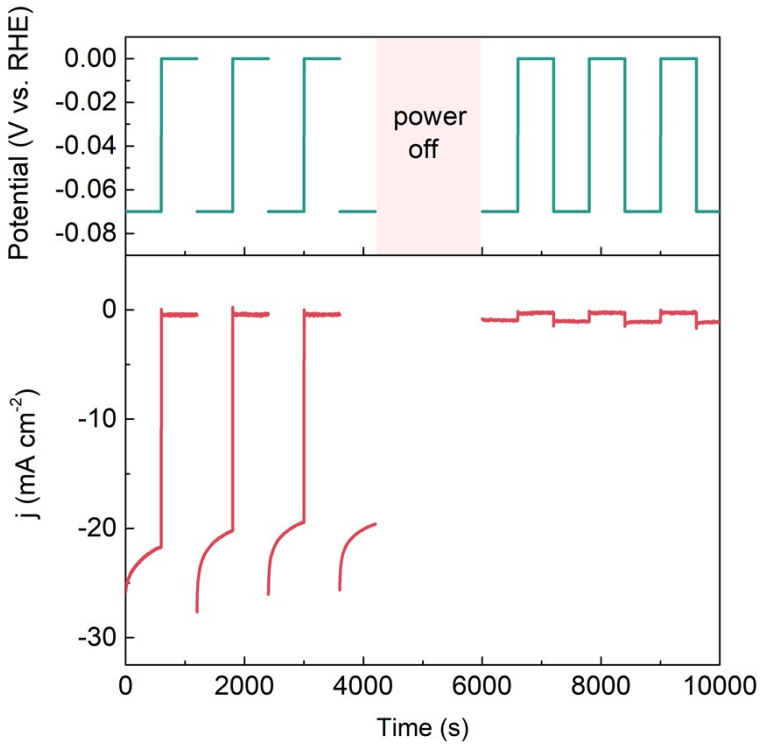

Fig. S6 Performance of the Ni–Cu–Mo catalyst in O_2-enriched 1.0 M KOH solution in intermittent operation. No cathodic protection was provided between 4200 and 6000 s.

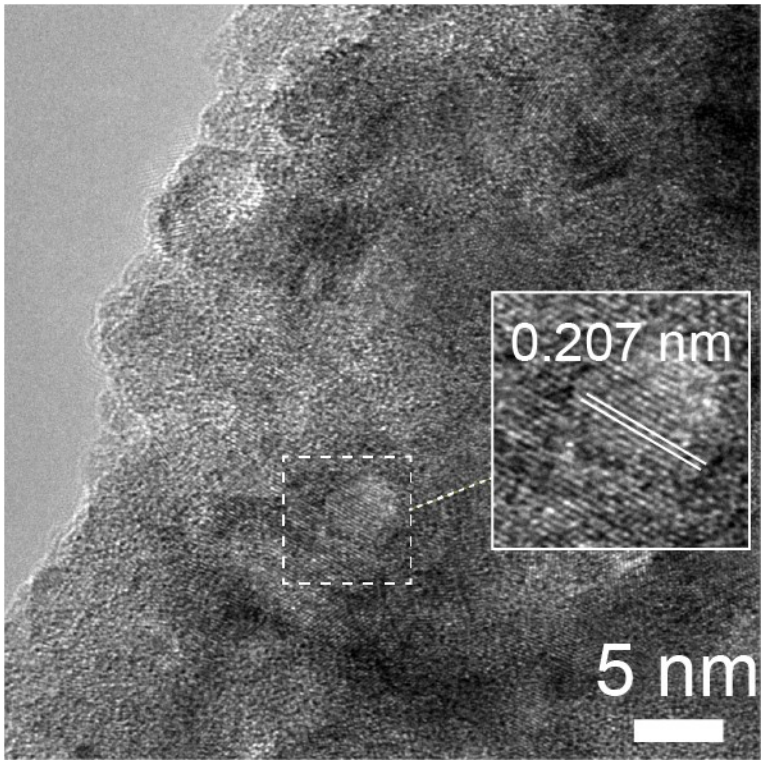

Fig. S7 High resolution TEM image of the Ni–Mo catalyst.

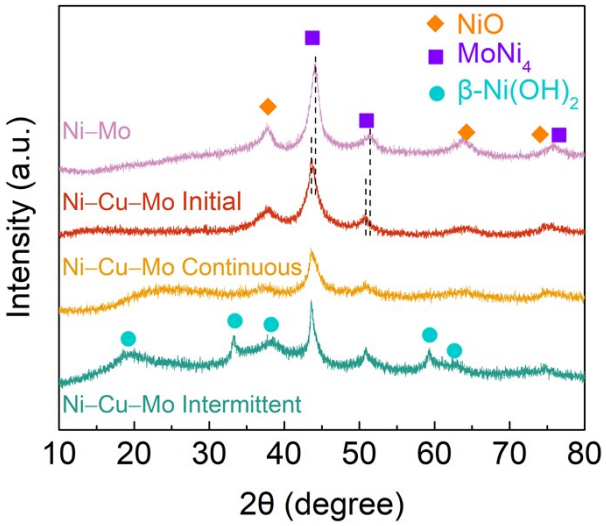

Fig. S8 XRD patterns of the Ni–Mo and Ni–Cu–Mo catalysts.

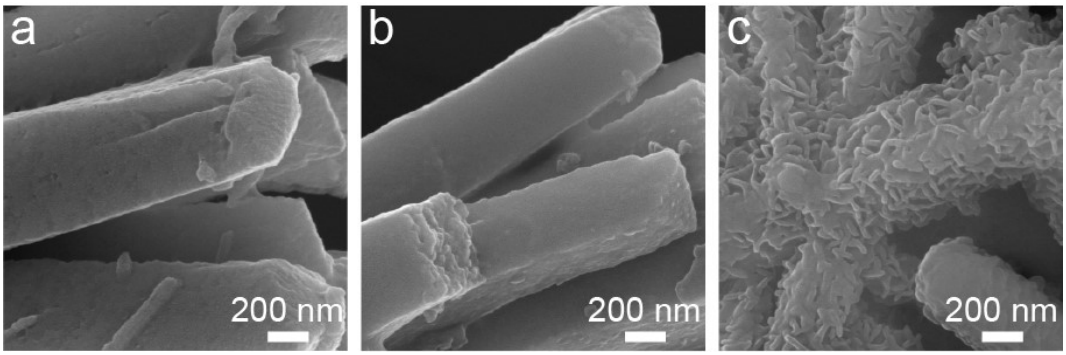

Fig. S9 SEM images of the Ni–Cu–Mo catalyst before (a) and after continuous (b) and intermittent (c) operations.

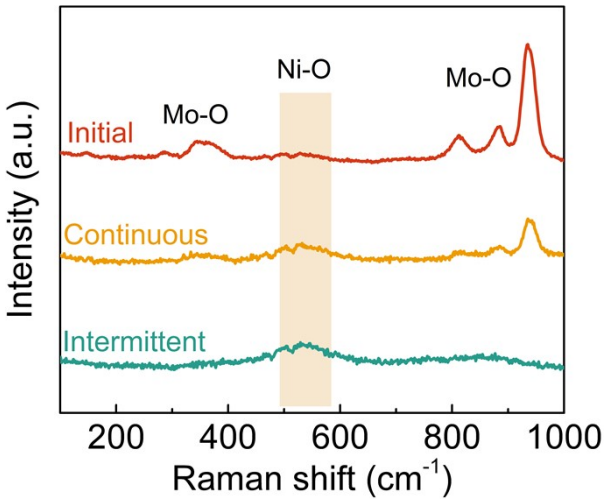

Fig. S10 Raman spectra of the Ni–Cu–Mo catalyst before and after continuous and intermittent operations.

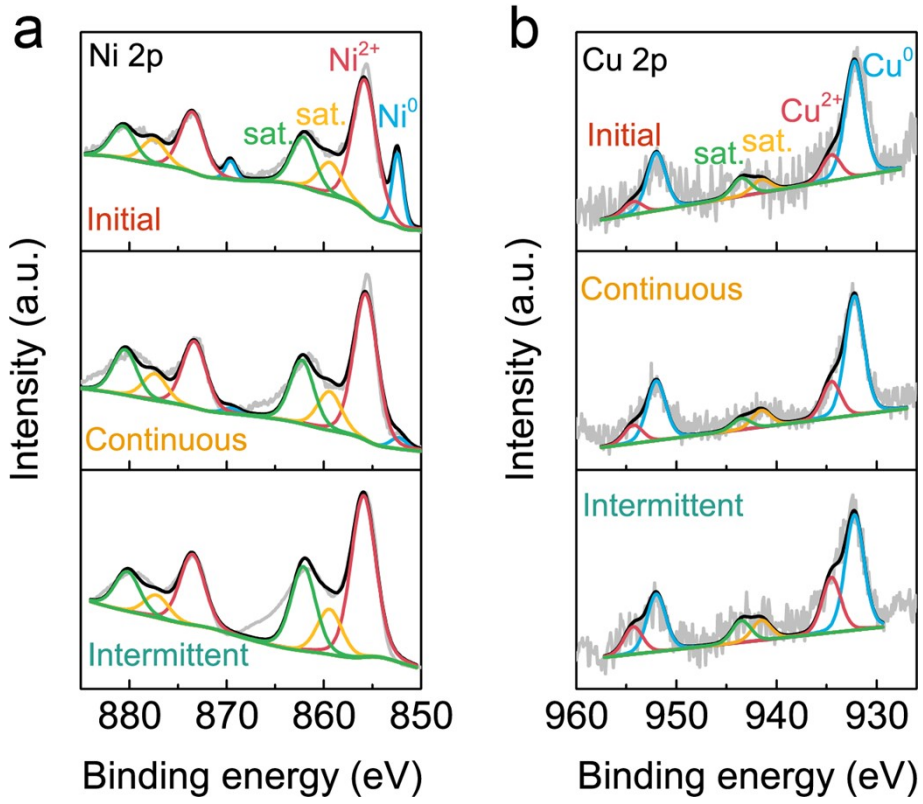

Fig. S11 The Ni 2p (a) and Cu 2p (b) XPS spectra of the Ni–Cu–Mo catalyst before and after continuous and intermittent operations.

References

1. J. R. McKone, B. F. Sadtler, C. A. Werlang, N. S. Lewis and H. B. Gray, *ACS Catal.*, 2013, **3**, 166-169.
2. M. Wang, H. Yang, J. Shi, Y. Chen, Y. Zhou, L. Wang, S. Di, X. Zhao, J. Zhong, T. Cheng, W. Zhou and Y. Li, *Angew. Chem. Int. Ed.*, 2021, **60**, 5771-5777.
3. J. Zhang, T. Wang, P. Liu, Z. Liao, S. Liu, X. Zhuang, M. Chen, E. Zschech and X. Feng, *Nat. Commun.*, 2017, **8**, 15437.
4. K. Chi, X. Tian, Q. Wang, Z. Zhang, X. Zhang, Y. Zhang, F. Jing, Q. Lv, W. Yao, F. Xiao and S. Wang, *J. Catal.*, 2020, **381**, 44-52.
5. J. Xiao, A. M. Oliveira, L. Wang, Y. Zhao, T. Wang, J. Wang, B. P. Setzler and Y. Yan, *ACS Catal.*, 2021, **11**, 264-270.